

Letter of Intent

Measurement of Dimuons from Drell-Yan Process with Polarized Proton Beams and an Internal Target at RHIC

May 24, 2010

K. N. Barish², M. L. Brooks⁵, A. Deshpande^{7,9}, N. Doshita¹¹, Y. Fukao⁶,
D. F. Geesaman¹, Y. Goto^{6,7}, M. Grosse Perdekamp³, T. Iwata¹¹,
X. Jiang⁵, K. Kondo¹¹, G. J. Kunde⁵, M. J. Leitch⁵, M. X. Liu⁵,
P. L. McGaughey⁵, Y. Miyachi^{10,11}, I. Nakagawa^{6,7}, K. Nakano^{6,10},
K. Okada⁷, J.-C. Peng³, P. E. Reimer¹, J. Rubin¹, N. Saito⁴, S. Sawada⁴,
R. Seidl^{6,7}, T.-A. Shibata¹⁰, A. Taketani^{6,7}, and K. Tanida⁸

¹ Argonne National Laboratory, Argonne, Illinois 60439, USA

² University of California - Riverside, Riverside, California 92521, USA

³ University of Illinois at Urbana-Champaign,
Urbana, Illinois 61801, USA

⁴ KEK, High Energy Accelerator Research Organization,
Tsukuba, Ibaraki 305-0801, Japan

⁵ Los Alamos National Laboratory, Los Alamos, NM 87545, USA

⁶ RIKEN, Institute of Physical and Chemical Research,
Wako, Saitama 351-0198, Japan

⁷ RIKEN BNL Research Center, Brookhaven National Laboratory,
Upton, NY 11973, USA

⁸ Seoul National University, Seoul 151-742, Korea

⁹ Stony Brook University, SUNY, Stony Brook, New York 11794, USA

¹⁰ Tokyo Institute of Technology, Tokyo 152-8551, Japan

¹¹ Yamagata University, Yamagata 990-8560, Japan

Abstract

In this Letter-of-Intent, we present the physics motivation and experimental consideration for a fixed-target polarized Drell-Yan dimuon experiment at RHIC. Using 250 GeV transversely polarized proton beams and an internal target at the IP2 area, dimuons from the Drell-Yan process can be detected using a spectrometer based on the existing Fermilab E906 spectrometer. The primary goal of the proposed experiment is to extract the Sivers parton distribution functions in the valence-quark region from the measurement of the Drell-Yan single-spin asymmetry (A_N). The sensitivity of the proposed fixed-target experiment will provide a stringent test of the QCD prediction that the Sivers function in the Drell-Yan process has an opposite sign to that in deep-inelastic scattering. The layout of the proposed experiment and results of some initial studies of the expected sensitivities are shown. Comparisons of the merits of the proposed experiment with other possible future polarized Drell-Yan experiments at various facilities are also presented.

Contents

1	Physics Motivations	4
1.1	Introduction	4
1.2	TMD functions and polarized Drell-Yan processes	4
1.3	Other physics topics	9
1.3.1	Unpolarized cross section measurement	9
1.3.2	Flavor asymmetry of the sea-quark polarization	9
1.3.3	Measurement of Boer-Mulders function	11
2	Experimental site and apparatus	12
2.1	Experimental apparatus	12
2.2	Experimental site	13
3	Beam Time Request	13
3.1	Phase-1: parasitic beam time	13
3.1.1	Option-1	13
3.1.2	Option-2 (beam dump mode)	14
3.2	Phase-2: dedicated beam time	14
4	Requirements	14
4.1	Requirement for the accelerator	14
4.2	Internal target	15
5	Experimental Sensitivities	15
5.1	Simulation study	15
5.2	Comparison with other experiments	17
5.2.1	COMPASS	17
5.2.2	GSI-FAIR (PAX and PANDA)	19
5.2.3	J-PARC	19
5.2.4	NICA	19
6	Estimated Cost and Schedule	19

1 Physics Motivations

1.1 Introduction

One of the most important topics in QCD physics is the spin structure of the nucleon. The composition of the nucleon's spin in terms of the quark/antiquark spin, the gluon spin, and the quark/gluon orbital angular momenta remains unclear and continues to be a most active area of research at various facilities including RHIC. In the last two decades, novel parton distributions involving the transverse spin and transverse momentum of quarks have been identified theoretically, and they are just beginning to be determined quantitatively in recent experiments.

Although the bulk of our current knowledge on the spin-averaged and spin-dependent parton distributions of the nucleon is acquired from lepton-induced inclusive deep-inelastic scattering (DIS) or semi-inclusive DIS reactions, complementary and often unique information can also be obtained from hadronic collisions. Well known examples include the Fermilab fixed-target E704 experiment measuring the single-spin asymmetry of hadrons produced with transversely polarized proton beams (and the extension of such measurements to much higher energies at RHIC) and the double-spin asymmetry measurements in longitudinally polarized p-p collision at RHIC. Unique information on the possible origins of the single-spin asymmetry as well as the gluon helicity distributions are obtained from these measurements.

The Drell-Yan process, in which a pair of charged leptons are produced in quark-antiquark annihilation, is an ideal tool for probing parton distributions. The mechanism of the Drell-Yan process is well understood and the absence of hadronization processes in the final state eliminates the uncertainties caused by the relatively poorly known fragmentation functions encountered in semi-inclusive DIS or hadron production in p-p collisions. The existence of polarized proton beams at RHIC is especially significant, since unique information on polarized parton distributions could be obtained in polarized Drell-Yan experiments. However, an important experimental challenge is that the Drell-Yan cross sections are relatively small, making a high-statistic measurement difficult. Indeed, the present luminosity at RHIC for polarized p-p collision has not yet allowed a viable experimental program to study the Drell-Yan process.

In this Letter-of-Intent, we discuss a new approach concerning a dedicated fixed-target Drell-Yan experiment at RHIC using an internal target. As discussed later, the anticipated luminosity will be adequate for a sensitive single-spin asymmetry Drell-Yan measurement to test a remarkable prediction on the non-universality of the so-called Sivers parton distribution function. [1] The proposed experimental approach will also allow a rich program addressing many important issues in spin physics using singly or doubly polarized Drell-Yan processes.

1.2 TMD functions and polarized Drell-Yan processes

The primary goal of the proposed experiment is to extract the Sivers function from the measurement of single-spin asymmetries in the Drell-Yan process using 250 GeV transversely polarized proton beams. Table 1 shows the leading twist distribution functions of the nucleon including intrinsic transverse momentum dependence based on a perturbative QCD approach specifying the different spin states of the nucleon and the partons.

	unpolarized parton	longitudinally-polarized parton	transversely-polarized parton
unpolarized nucleon	f_1		h_1^\perp
longitudinally-polarized nucleon		g_1	h_{1L}^\perp
transversely-polarized nucleon	f_{1T}^\perp	g_{1T}	h_1, h_{1T}^\perp

Table 1: Leading twist transverse momentum dependent distribution functions of the nucleon.

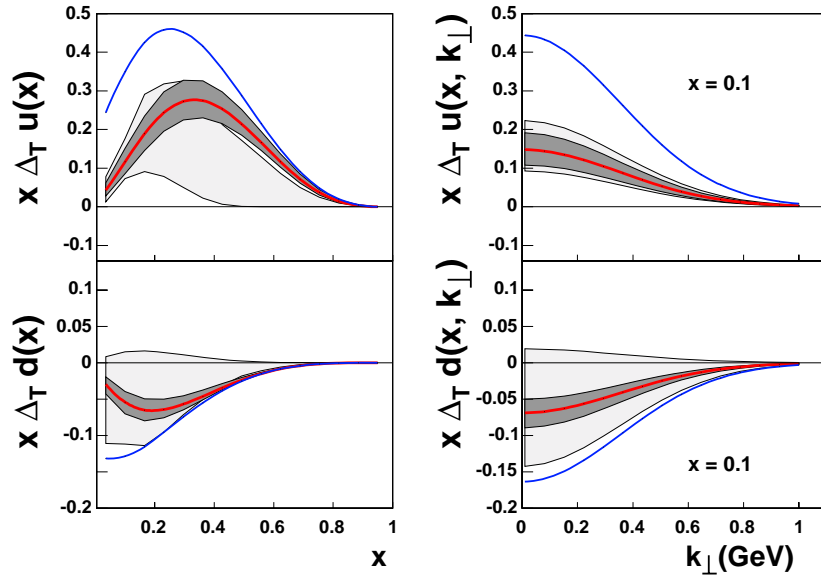


Figure 1: Transversity functions of u-quarks and d-quarks obtained in the global fit from [6].

Diagonal elements of the table (f_1 , g_1 , and h_1) show leading-twist light-cone distribution functions which survive upon integration of transverse momenta. The distribution function h_1 is known as the transversity. [2] It is the remaining leading-order polarized distribution function of the nucleon, and shows the distribution of the transverse-spin of partons inside a transversely polarized nucleon. First transversity distributions were extracted by a global fit of the Collins asymmetries measured at HERMES [3] on a transversely polarized proton target, COMPASS [4] on a transversely polarized deuteron target and the Collins fragmentation functions measured by the Belle experiment [5]. As an example Fig. 1 shows the transversity distribution functions of u-quarks and d-quarks obtained by the global fit of Anselmino's group [6].

The transversity parton distributions can also be probed in Drell-Yan experiments. As pointed out some time ago [7], the double transverse spin asymmetry in polarized Drell-Yan, A_{TT} , is proportional to the product of transversity distributions, $h_1(x_q)h_1(x_{\bar{q}})$. A_{TT} could be measured at RHIC in the future with a transversely polarized proton beam colliding with either another transversely polarized proton beam or target. Such measurements would lead to the determination of the antiquark transversity distributions, $h_1(x_{\bar{q}})$, which are difficult to isolate from the semi-inclusive DIS experiments. It is worth noting that information on the antiquark transversity distributions are required to determine the nucleon tensor charge, for which lattice QCD calculations are already available [8].

The other elements in Table 1 correspond to transverse-momentum dependent (TMD) distribution functions which would not survive upon integration of all observed transverse momenta. The distribution functions f_{1T}^\perp and h_1^\perp are known as Sivers and Boer-Mulders functions which describe unpolarized partons in a transversely polarized nucleon and transversely-polarized partons in an unpolarized nucleon respectively. They vanish at tree-level in a T-reversal invariant model (T-odd) and can only be non-zero when initial or final state interactions cause an interference between different helicity states.

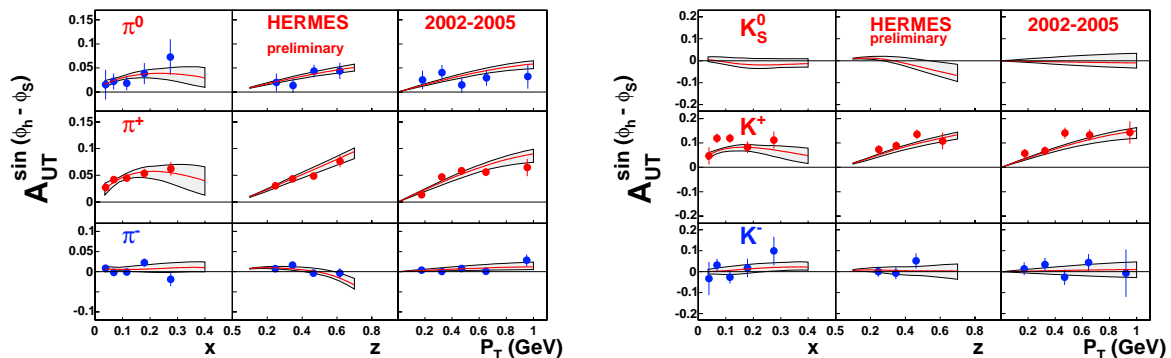


Figure 2: Results of the global fit for the HERMES Sivers asymmetry of pions and kaons by Anselmino's group [11].

The Sivers asymmetry has been determined in semi-inclusive DIS in the HERMES [3],[9] and COMPASS [4] experiments by decomposing the initial-state effect (Sivers asymmetry) and the final-state effect (Collins asymmetry) using their different azimuthal angular dependencies. Both experiments have already measured multipoint of the Sivers

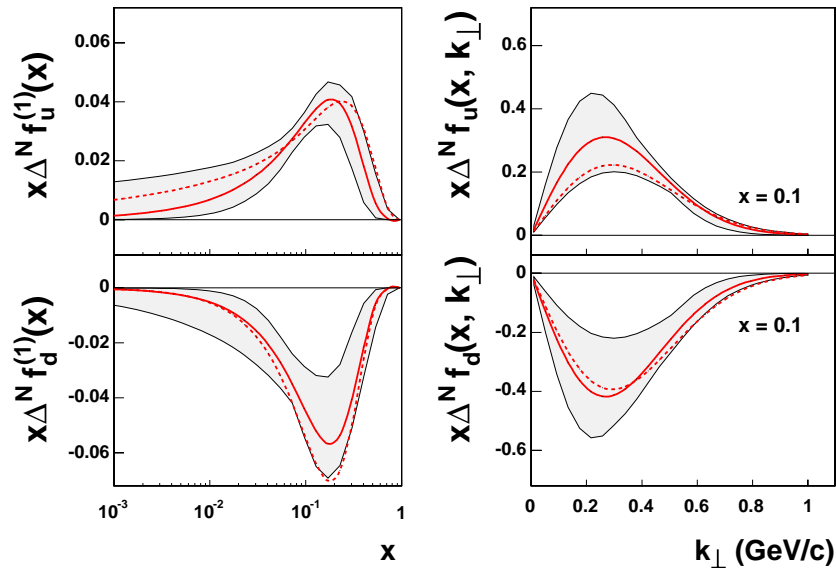


Figure 3: Siverts functions of u-quark and d-quark at the scale $Q^2 = 2.4 \text{ (GeV}/c)^2$ obtained in the global fit [11].

asymmetry in the momentum fraction region of $0.005 < x < 0.3$ with smaller than 1% level error bars as shown in Fig. 2. The Siverts function has been obtained from a global fit of the Siverts asymmetry measured at HERMES (proton target) and COMPASS (deuteron target) by several theory groups [10, 11]. Fig. 2 also shows results of the global fit for the HERMES Siverts asymmetry of pions and kaons by Anselmino’s group and Fig. 3 shows Siverts functions of u-quark and d-quark obtained in the global fit. [11]

One important property of the Siverts function found in the theoretical studies is its “non-universality”. The Siverts function contributes with opposite sign to the transverse-spin asymmetries in the DIS process and the Drell-Yan process [12]:

$$f^{Siverts}(x, k_{\perp})|_{DY} = -f^{Siverts}(x, k_{\perp})|_{DIS}. \quad (1)$$

This is a fundamental QCD prediction based on gauge invariance and its verification is an important milestone for the field of hadron physics. It allows to test nonperturbative aspects of QCD and the concept of factorization including transverse-momentum dependence for analyzing hard-scattering reactions.

This consequence of a sign change is based on the concept that in order to have a nonzero Siverts effect rescattering of the quarks and the hadron remnants are required as those create the required interference. This rescattering process can be either attractive or repulsive in the two processes and thus gives rise to the opposite signs. In order to have an intuitive understanding of Eq.(1), we consider a “toy” process as shown in Fig. 4. A transversely polarized charge-less “hadron” consists of particles with electric charges +1 and -1, The DIS-like process in the lepton scattering shown in Fig. 4(a) has a final-

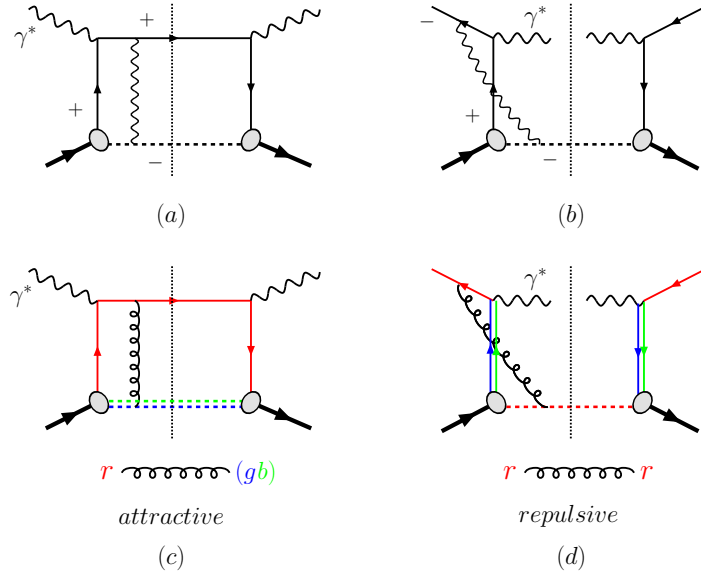


Figure 4: (a),(b) Simple QED example for process-dependence of the Sivers functions in DIS and the Drell-Yan process. (c),(d) Same for QCD.

state interaction with remnant partons in the proton by exchange of a photon. As the electric charges of the two interacting particles are opposite, this final-state interaction is *attractive*. The Drell-Yan process in the hadron reaction shown in Fig. 4(b) has an initial-state interaction with remnant partons in the proton by exchange of a photon. These have identical charges, and the interaction is *repulsive*. As a result, the spin-effect in the Drell-Yan process needs to be of opposite sign as that in the DIS process. These simple models are generalized to true hadronic scattering in QCD where the measurement process needs to have an initial-state or final-state interaction with remnant partons in the proton through a gluon exchange as shown in Fig. 4(c) and (d).

It is now crucial to investigate the Sivers transverse-spin asymmetry in the Drell-Yan process in order to compare it with that from the DIS process and to test the “non-universality” shown in Eq.(1). This has become one of the top priorities for the worldwide hadronic physics community. We need to measure the asymmetry in the Drell-Yan process to collect a significant amount of statistics to be comparable with that of the DIS data.

In the Drell-Yan process one measures the Sivers function in single transverse spin asymmetries A_{UT} , where only one of the initial nucleons is transversely polarized. Similar to the case of DIS, where one has to disentangle two single spin asymmetries (Sivers and Transversity with Collins) also in the Drell Yan process two competing single spin asymmetries exist, Sivers as well as Transversity with the Boer-Mulders function [13, 14]. However also in the Drell-Yan process those two can be separated via its different dependencies on the azimuthal angles of the lepton production plane (ϕ) and the nucleon’s spin vector relative to the two hadron plane (ϕ_S). Following [13] the Sivers component is proportional to a $\sin(\phi - \phi_S)$ modulation while Transversity with the Boer-Mulders

function is proportional to a $\sin(\phi + \phi_S)$ modulation:

$$\begin{aligned} \frac{d\sigma}{d\Omega d\phi_S dx_1 dx_2 d^2\mathbf{q}_T} &\propto \frac{\alpha^2}{12Q^2} \Sigma_q e_q^2 \times \{ \dots \\ &+ (1 + \cos^2 \theta) \sin(\phi - \phi_S) \mathcal{F} [\dots f_1^q f_{1T}^{\perp q}] \\ &+ (\sin^2 \theta) \sin(\phi + \phi_S) \mathcal{F} [\dots h_1^{q\perp} h_1^q] \} \quad , \end{aligned} \quad (2)$$

where $\mathcal{F}[\]$ corresponds to the convolution integrals over functions of the corresponding transverse momenta (omitted here).

It is worth noting that the first COMPASS data from a transverse-spin run in 2007 with a polarized proton target shows small Sivers asymmetries compatible with zero over the full x -range for both positive and negative hadrons [15]. This would be in contradiction to the HERMES measurements and cast some doubt on the existence of the Sivers function. Since then an updated analysis shows some nonzero asymmetries [16]. While still smaller than HERMES and possibly with an unexpected W dependence it returns confidence in the existence of the Sivers function now being observed in two independent experiments. The COMPASS experiment is currently running again with a transversely-polarized proton target and plan to improve statistics by a factor 3 over the whole x -range.

1.3 Other physics topics

1.3.1 Unpolarized cross section measurement

Since the collision energy of the fixed-target experiment is lower than that of the collider experiment, it is important to discuss the availability of the perturbative QCD based on the unpolarized Drell-Yan cross section. The perturbative QCD calculation has to be controlled theoretically in the energy scale of the fixed-target experiment, and the measured cross section has to be explained by the perturbative QCD before discussion the polarized results theoretically. The theory calculation requires not only the next-to-leading order (NLO) and next-to-next-to-leading order (NNLO) corrections, but also the next-to-leading log (NLL) and next-to-next-to-leading log (NNLL) corrections for consistent understanding of the cross section [17].

The left panel of Fig. 5 shows the cross section calculation with these corrections, and the right panel shows the K -factors, the cross section normalized by the leading order (LO) calculation. The results with the NLL and NNLL correction show good convergence of the calculation.

Figure 6 shows a predicted cross section at the RHIC fixed-target experiment in the scaling form which is compared with previous measurements mostly with higher collision energies. At high τ , the theory calculation predicts higher cross section measurement caused by the high K -factor than the previous measurements.

1.3.2 Flavor asymmetry of the sea-quark polarization

To obtain the total quark and gluon contribution to the nucleon spin with high precision, it is important to know the flavor-sorted sea-quark contribution to the nucleon spin directly. Because the Q^2 evolution of the quark and gluon distribution mixes them, uncertainties of the flavor-sorted sea-quark distribution propagate to uncertainties of the quark and gluon

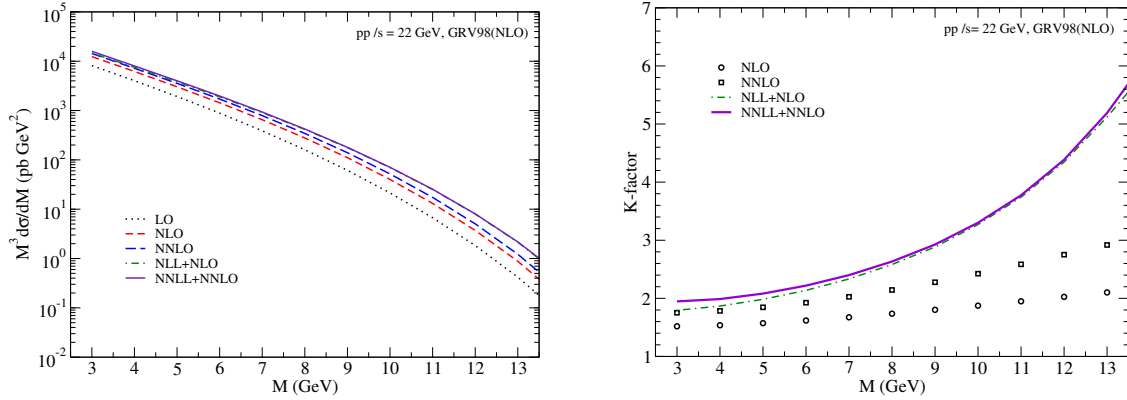


Figure 5: The left panel shows the cross section calculation by the perturbative QCD with NLO, NNLO, NLL, and NNLL corrections, and the right panel shows the K -factors, the cross section normalized by the leading order (LO) calculation.

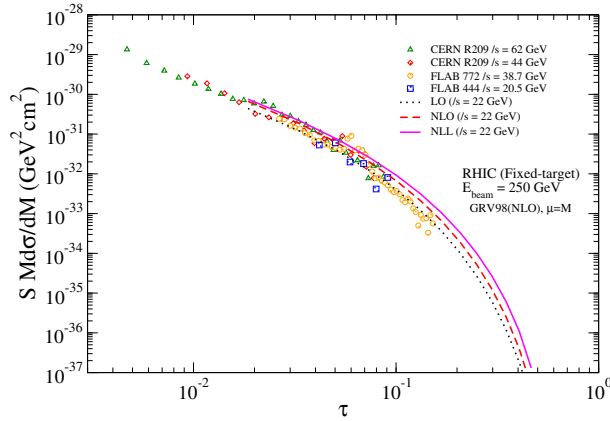


Figure 6: Predicted cross section at the RHIC fixed-target experiment in the scaling form which is compared with previous measurements mostly with higher collision energies, where $\tau = M^2/s$.

distributions. It is also important to know the helicity distribution of the sea-quark at high- x to give an additional input to the physics of the flavor asymmetry of the sea-quark distribution shown in the unpolarized distribution by the Fermilab E866 experiment.

With a thick enough polarized internal target, or storage-cell target (both proton and deuteron), and spin rotator magnets which makes the beam longitudinally polarized, the flavor asymmetry measurement of the sea-quark polarization can be measured. The flavor asymmetry of the sea-quark polarization has been and will be measured by DIS experiments and RHIC weak boson measurements. The results will be compared.

1.3.3 Measurement of Boer-Mulders function

As discussed above, another T-odd distribution function is the Boer-Mulders function, $h_1^\perp(x, k_\perp)$, which signifies the correlation between k_\perp and the quark transverse spin, s_\perp , in an unpolarized nucleon. The Boer-Mulders function is the chiral-odd analog of the Sivers function and also owes its existence to the presence of initial/final state interactions. While the Sivers function is beginning to be quantitatively determined from the DIS experiments, very little is known about the Boer-Mulders function so far.

Several model calculations have been carried out for the Boer-Mulders functions. In the quark-diquark model, it was shown that the Boer-Mulders functions are identical to the Sivers functions when only the scalar diquark configuration is considered. More recently, calculations taking into account both the scalar and the axial-vector diquark configurations found significant differences in flavor dependence between the Sivers and Boer-Mulders functions. In particular, the u and d valence quark Boer-Mulders functions are predicted to be both negative, while the Sivers function is negative for the u and positive for the d valence quarks. Other calculations using the MIT bag model, the relativistic constituent quark model, the large- N_c model, and lattice QCD also predict negative signs for the u and d valence Boer-Mulders functions. The model predictions for the same signs of the u and d Boer-Mulders functions remain to be tested experimentally. Furthermore, the striking prediction that the T-odd Boer-Mulders functions in the DIS process will change their signs for the Drell-Yan process also awaits experimental confirmation.

The Boer-Mulders functions can be extracted from the azimuthal angular distributions in the unpolarized Drell-Yan process, $h_1 h_2 \rightarrow l^+ l^- X$. The general expression for the Drell-Yan angular distribution is

$$\frac{d\sigma}{d\Omega} \propto 1 + \lambda \cos 2\theta + \mu \sin 2\theta \cos \phi + \frac{\nu}{2} \sin 2\theta \cos 2\phi, \quad (3)$$

where θ and ϕ are the polar and azimuthal decay angle of the l^+ in the dilepton rest frame. Boer showed that the $\cos 2\phi$ term is proportional to the convolution of the quark and antiquark Boer-Mulders functions in the projectile and target. The first measurement of the $\cos 2\phi$ dependence of the Drell-Yan process was recently reported for the $p + p$ and $p + d$ interactions at 800 GeV/c [18]. Recent analysis of the Drell-Yan data by Lu and Schmidt has extracted the Boer-Mulders functions, and has predicted $\cos 2\phi$ asymmetries in future experiments [19]. Clearly, new measurements covering different kinematic region could be performed using the apparatus proposed here.

The polarized proton beams at RHIC offers another independent technique to measure the Boer-Mulders function. The polarized cross section of the Drell-Yan process measured with transversely polarized beams is written as Eq.(2). The $\sin(\phi - \phi_S)$ term of the

transverse single-spin measurement gives the transversity distribution combined with the Boer-Mulders function. This allows an independent measurement for both the transversity distribution and the Boer-Mulders function.

2 Experimental site and apparatus

2.1 Experimental apparatus

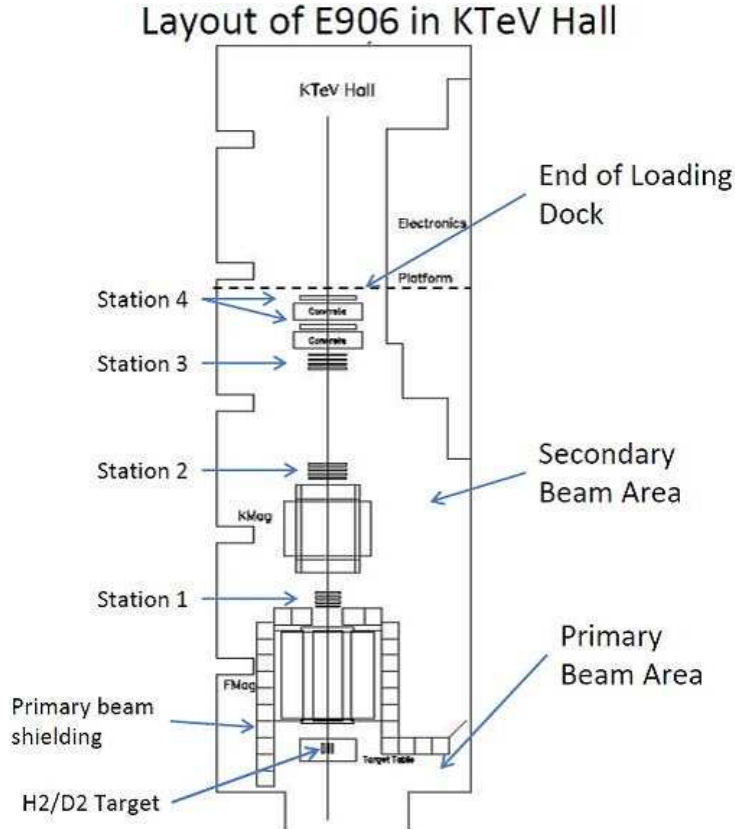


Figure 7: Layout of the E906 spectrometer.

The experimental apparatus is similar to the one used in a series of experiment at Fermilab with extracted beams (E605, E772, E789, E866, and E906). The FNAL-E906 spectrometer comprises a solid iron focusing dipole magnet containing the beam dump, followed by a large open aperture dipole for precise momentum determination. Multi-wire proportional and drift chambers between the first two magnets as well as after the second dipole provide tracking information, supplemented by scintillation hodoscopes used primarily for fast triggering. A final large iron absorber instrumented with proportional tubes provides muon identification. Layout of the FNAL-E906 spectrometer are shown in Fig. 7. We expect to use as many of the detector elements and electronics as possible from the FNAL-E906 experiment available after the completion of the experiment in 2013.

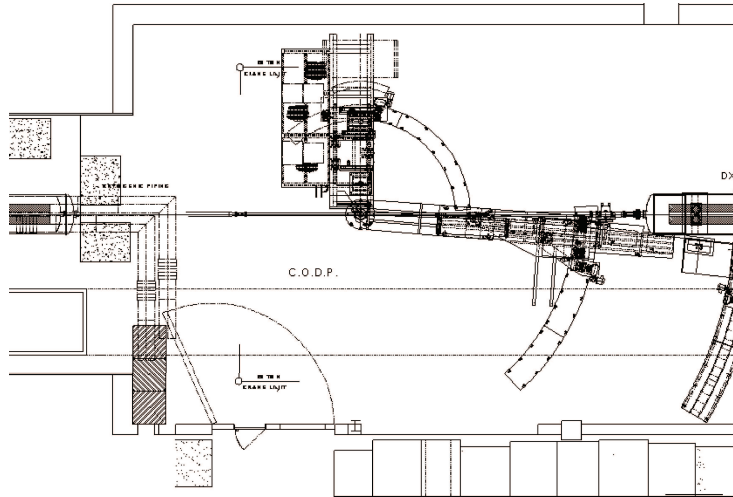


Figure 8: IP2 area (with BRAHMS).

2.2 Experimental site

The IP2 area (previous BRAHMS site, shown in Fig. 8) is the candidate experimental site. It has an available space of ± 7 m of the nominal interaction point (or 14 m in total). We expect the target position can be set anywhere in this space. There is about 1.7 m space from the floor to the beam pipe which may need minor civil engineering work to fit the FNAL-E906 detector, especially for downstream large detectors.

3 Beam Time Request

We plan to have two phases of the beam-time request, parasitic beam time with collider experiments as a phase-1, and dedicated beam time as a phase-2.

3.1 Phase-1: parasitic beam time

There are two possibilities for parasitic running of this experiment. Each presents different constraints. Both options are discussed below. We will additionally discuss these options with the accelerator group to determine which is the better option, or if they can be combined in some way.

3.1.1 Option-1

We request a beam intensity of 2×10^{11} / bunch with 112 bunches or ~ 10 MHz, which corresponds to 2×10^{18} /s. We will use a cluster-jet target or pellet target with a thickness of 10^{15} atoms / cm^2 . The thickness is about 50 times thinner than RHIC CNI carbon target, and we hope it is acceptable as a parasitic experiment with collider experiments. It corresponds to a luminosity of 2×10^{33} $\text{cm}^{-2}\text{s}^{-1}$. We can accumulate 10,000 pb^{-1} luminosity with 5×10^6 seconds, approximately 8 week, or 3 years of beam time by considering efficiency and live time. Since the reaction rate can be estimated to be 10^8 /s = 100 MHz, the beam lifetime can be very naively estimated to be $2 \times 10^{11} \times 112$ bunches / 10^8

= 2×10^5 seconds. There will be more factors to make the beam lifetime shorter, but we expect the beam lifetime is long enough for the other experiments.

3.1.2 Option-2 (beam dump mode)

This option is feasible if we can use an internal-target with a thickness of 10^{17} atoms / cm^2 . We request our beam time at the end of every fill after stopping collider experiments and dumping one beam which is not used by us. Assuming a beam intensity of 10^{11} / bunch with 112 bunches, we expect to use 20% of beam particles by reaction with the target which corresponds to 40 pb^{-1} . It will take about 1,000 seconds depending on how fast the beam dumps. We request 250 fills to accumulate $10,000 \text{ pb}^{-1}$.

3.2 Phase-2: dedicated beam time

We request a beam intensity of 2×10^{11} / bunch with 168 bunches (as assumed at eRHIC) or ~ 15 MHz, which corresponds to 3×10^{18} /s. (Otherwise, we require 1.5 times longer beam time.) We will use a pellet target or solid target with a thickness of 10^{16} atoms / cm^2 . The thickness is about 5 times thinner than RHIC CNI carbon target. It corresponds to a luminosity of $3 \times 10^{34} \text{ cm}^{-2}\text{s}^{-1}$. We can accumulate $30,000 \text{ pb}^{-1}$ luminosity with 10^6 seconds, approximately 2 weeks, or 8 weeks of beam time by considering efficiency and live time. Since the reaction rate can be estimated to be 1.5×10^9 /s = 1.5 GHz, the beam lifetime can be very naively estimated to be $2 \times 10^{11} \times 168 \text{ bunches} / 1.5 \times 10^9 = 2 \times 10^4$ seconds, or 6 hours. There will be more factors to make the beam lifetime shorter. Special short-interval operation will be necessary.

4 Requirements

4.1 Requirement for the accelerator

To meet the requirements of polarized Drell-Yan experiment, there are issues to be cleared.

- Higher beam intensity is required, *e.g.* with 1.5-times more number of bunches (112 bunches \rightarrow 168 bunches as assumed at eRHIC, otherwise, we require 1.5 times longer beam time).
- Appropriate beam lifetime needs to be kept. The beam lifetime can be very naively estimated by dividing number of beam particles with a reaction rate, but it is also affected by beam blow-up issue, etc. Collider experiments will require not only the beam lifetime but also high quality beam (*e.g.* low background).
- The beam is required to be restored on axis after passing through the two bending magnets in the experimental apparatus. In the parasitic operation with collider experiments, both beams need to be restored on axis, one hitting the internal target and the other displaced by about 1 cm.
- There may be a radiation issue to achieve the required beam intensity and luminosity. We hope this will be addressed by appropriate radiation shielding.
- Peak rate of the total reactions?

4.2 Internal target

The internal target needs to be optimized to give the maximum luminosity. There are following technology choices.

cluster-jet target A prototype of the high-intense cluster-jet source for the PANDA experiment is currently in operation at the University Münster and allows for hydrogen target thickness in the order of 8×10^{14} atoms/cm². Current improvements are expected to lead to even higher numbers. Instead of hydrogen also deuterium can be used as cluster material. Additionally, the use of heavier gases is possible to provide nuclear targets. [20]

pellet target A first-generation pellet target was developed in Uppsala with an average thickness of 10^{16} atoms/cm² and is in use with the WASA-at-COSY experiment. A more sophisticated target, being the prototype of the later PANDA pellet target, is available at the Forschungszentrum Jülich. It has been developed in collaboration with two groups from Moscow, ITEP and MPEI. With this target also pellets from Nitrogen and Argon have been produced. Other materials, like Deuterium or heavy noble gases, are also feasible. [20]

In the parasitic operation, 10^{15} /cm² thickness is necessary to achieve $L = 2 \times 10^{33}$ cm⁻²s⁻¹. In order to achieve this luminosity, pellet target or cluster-jet target is necessary. In the dedicated operation, 10-times larger thickness, 10^{16} /cm², is expected.

5 Experimental Sensitivities

5.1 Simulation study

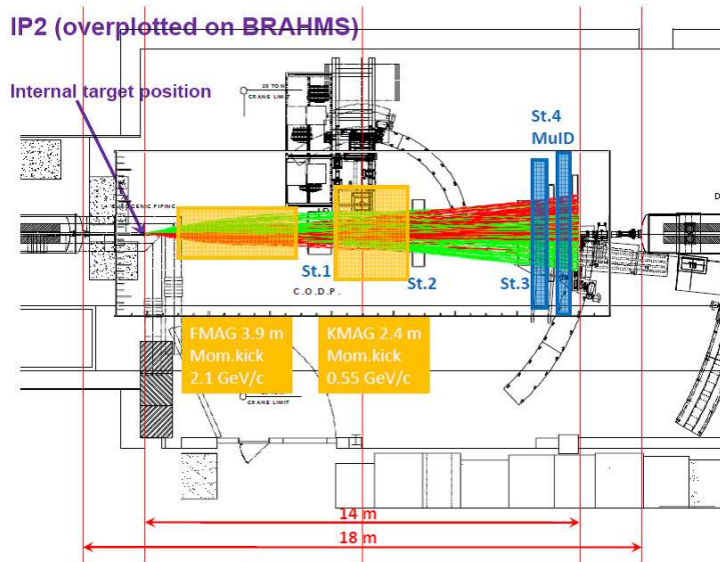


Figure 9: IP2 area (with BRAHMS).

A fast Monte Carlo simulation with an experimental apparatus fitted in the IP2 area has been performed to evaluate the kinematic acceptance and yield of the experiment. Assumptions of the experimental components and detector elements are based on the FNAL-E906 experiment apparatus, but restriction of the size of the IP2 area in the beam direction must be considered. Figure 9 shows geometry of the experimental apparatus fitted in the IP2 area, and the sample dimuon tracks generated in the simulation.

The total length of the E906 apparatus is about 25 meter, but the size of the IP2 area is about 14 meter in the beam direction. In order to accommodate the detector apparatus in this area, the size of the first dipole magnet is assumed to have 3.9 meter size in the beam direction with 2.1 GeV/ c momentum kick instead of the size of the E906 first magnet with about 5 meter size and 2.5 GeV/ c momentum kick. The second dipole magnet for the momentum analysis is assumed to have 2.4 meter size in the beam direction with 0.55 GeV/ c momentum kick. The geometrical momentum resolution of the spectrometer is $6 \times 10^{-4} \times p$ (GeV/ c).

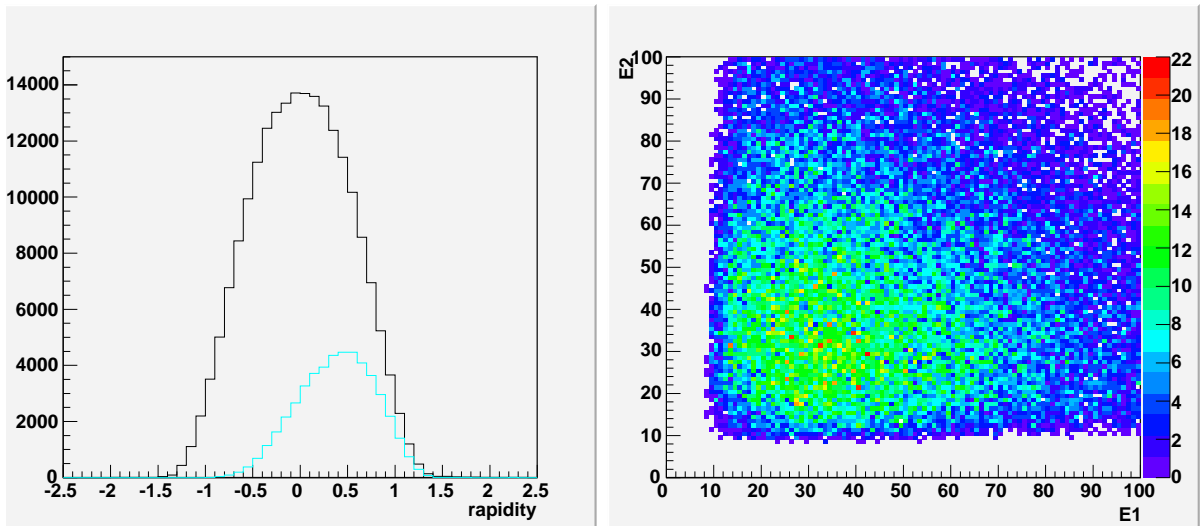


Figure 10: Results of the fast Monte Carlo simulation with PYTHIA the internal-target experiment at RHIC. The left panel shows a rapidity distribution of dimuons and the right panel shows a scattering plot of energies of dimuon pairs. The muon energy cut by the spectrometer is shown to be about 10 GeV.

Results of the fast Monte Carlo simulation with PYTHIA for the internal-target experiment at $E_{beam} = 250$ GeV or $\sqrt{s} = 22$ GeV are shown. By assuming a luminosity of $10,000 \text{ pb}^{-1}$, we estimate about 50,000 Drell-Yan events will be collected at the dimuon invariant mass region $4.5 < M_{\mu\mu} < 8$ GeV. The rapidity distribution of dimuons is shown in the left panel of Fig. 10. The muon energy cut by the spectrometer is shown to be about 10 GeV in the right panel of Fig. 10.

Figure 11 shows the experimental coverage of x_1 , the momentum fraction of the polarized proton beams. The sensitive x region of the Sivers function ($f_{1T}^\perp(x)$) measurement is 0.2 - 0.6 which has an overlap with the measured region by the DIS experiments ($x < 0.3$) and cover higher- x region with better sensitivity. We want to make the x -coverage as low as possible to compare with the DIS data with better sensitivity. We need more optimization of the detector geometry and acceptance so that it covers the lower- x region, and

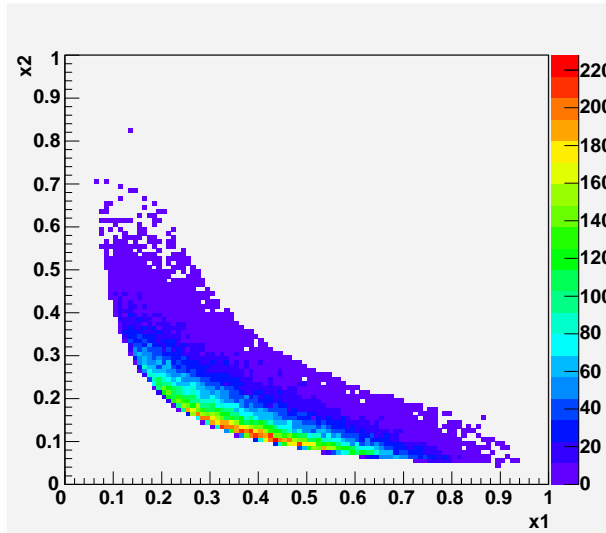


Figure 11: The experiment coverage of x_1 and x_2 , the momentum fraction of the polarized proton beams and the target protons.

simulation of physics background from charm, etc. and evaluation of background rate with the GEANT simulation.

By using a transversely polarized beam, measurement of single-spin asymmetry, or A_N :

$$A_N = \frac{\sigma_L - \sigma_R}{\sigma_L + \sigma_R}, \quad (4)$$

gives the Sivers function. Figure 12 shows the A_N integrated over transverse momentum $0 < q_T < 1$ GeV/ c of the virtual photon and dimuon mass range $4.5 < M_{\mu^+\mu^-} < 8$ GeV calculated with the Sivers function [21, 22]. Expected statistical sensitivities are calculated for 10,000 pb $^{-1}$ in phase-1 and 40,000 pb $^{-1}$ in phase-1 + phase-2 assuming 70% polarization. By these measurements, we will be able to study not only the sign of the Sivers function but also the shape of the function.

5.2 Comparison with other experiments

Table 2 summarizes comparison between RHIC Drell-Yan experiments and other experiments.

5.2.1 COMPASS

In the COMPASS experiment, polarized Drell-Yan experiment with charged pion beams and polarized targets are proposed. It proposes to use 160-GeV (or $\sqrt{s} = 17.9$ GeV) π^+ and π^- beams with 6×10^7 /s beam intensity and a polarized hydrogen target (H-butanol, NH $_3$, or 7 LiH). A luminosity corresponds to 2×10^{33} cm $^{-2}$ s $^{-1}$. It also proposes to use a polarized deuterium target (D-butanol or 6 LiD). The experiment is proposed to start in 2012, and collect 200,000 Drell-Yan events for 2-year data taking at invariant mass region $4 < M_{\mu\mu} < 9$ GeV.

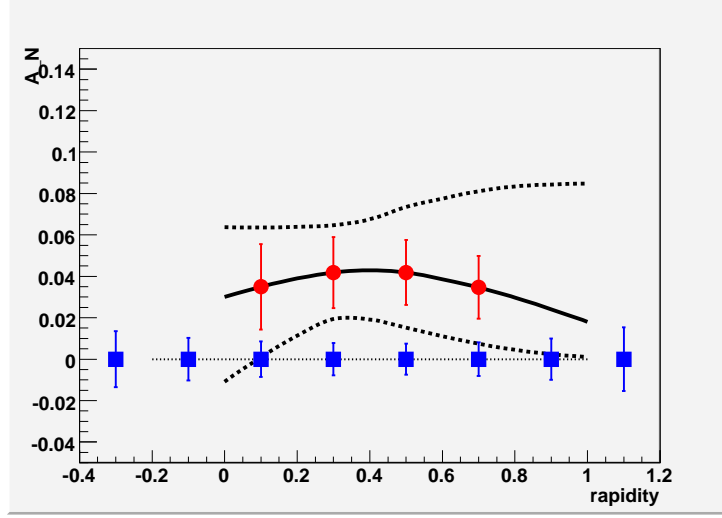


Figure 12: Drell-Yan A_N integrated over $0 < q_T < 1$ GeV/ c and $4.5 < M_{\mu^+\mu^-} < 8$ GeV. Expected statistical sensitivities for $10,000 \text{ pb}^{-1}$ (red circles) in phase-1 and $40,000 \text{ pb}^{-1}$ (blue squares) in phase-1 + phase-2 are shown.

experiment	particles	energy	x_1 or x_2	luminosity
COMPASS	$\pi^\pm + p \uparrow$	160 GeV $\sqrt{s} = 17.4$ GeV	$x_2 = 0.2 - 0.3$	$2 \times 10^{33} \text{ cm}^{-2}\text{s}^{-1}$
COMPASS (low mass)	$\pi^\pm + p \uparrow$	160 GeV $\sqrt{s} = 17.4$ GeV	$x_2 \sim 0.05$	$2 \times 10^{33} \text{ cm}^{-2}\text{s}^{-1}$
PAX	$p \uparrow + \bar{p}$	collider $\sqrt{s} = 14$ GeV	$x_1 = 0.1 - 0.9$	$2 \times 10^{30} \text{ cm}^{-2}\text{s}^{-1}$
PANDA (low mass)	$\bar{p} + p \uparrow$	15 GeV $\sqrt{s} = 5.5$ GeV	$x_2 = 0.2 - 0.4$	$2 \times 10^{32} \text{ cm}^{-2}\text{s}^{-1}$
J-PARC	$p \uparrow + p$	50 GeV $\sqrt{s} = 10$ GeV	$x_1 = 0.5 - 0.9$	$10^{35} \text{ cm}^{-2}\text{s}^{-1}$
NICA	$p \uparrow + p$	collider $\sqrt{s} = 20$ GeV	$x_1 = 0.1 - 0.8$	$10^{30} \text{ cm}^{-2}\text{s}^{-1}$
RHIC Internal Target phase-1	$p \uparrow + p$	250 GeV $\sqrt{s} = 22$ GeV	$x_1 = 0.2 - 0.6$	$2 \times 10^{33} \text{ cm}^{-2}\text{s}^{-1}$
RHIC Internal Target phase-2	$p \uparrow + p$	250 GeV $\sqrt{s} = 22$ GeV	$x_1 = 0.2 - 0.6$	$3 \times 10^{34} \text{ cm}^{-2}\text{s}^{-1}$

Table 2: Comparison with other experiments.

The Drell-Yan experiment with π^- (π^+) beam is sensitive to d-quark (u-quark) in the nucleon target, and the sign of the asymmetry for π^- (π^+) beam is given by the sign of the Sivers function of d-quark (u-quark). The experiment at lower mass region, $2 < M_{\mu\mu} < 2.5$ GeV, below the J/ψ and above the ρ resonance peaks, where data should be much more abundant, may also be performed.

5.2.2 GSI-FAIR (PAX and PANDA)

The PAX experiment is an asymmetric collider experiment with 15-GeV polarized antiproton and 3.5-GeV polarized proton proposed at GSI-FAIR ($\sqrt{s} = 14.4$ GeV). The polarized Drell-Yan measurement at PAX can give Sivers functions of partons in the polarized antiproton and in the polarized proton.

At GSI-FAIR, there is another experiment with antiproton beams, PANDA experiment. The polarized Drell-Yan measurement at PANDA with a polarized internal target may be performed at low-mass region.

5.2.3 J-PARC

There is a proposed dimuon experiment with 50-GeV proton beams at J-PARC ($\sqrt{s} = 10$ GeV). There is also a proposal of the acceleration of polarized proton beams to 30-50 GeV at the J-PARC facility. Polarized proton beam acceleration with two partial helical Siberian snakes is shown to be feasible in discussion with J-PARC and BNL accelerator physicists. [23] If the polarized proton beams are made available, the polarized Drell-Yan measurement can be performed.

5.2.4 NICA

The Spin-Purpose Detector (SPD) project is proposed at the second interaction point of the NICA collider. The purpose of the experiment is the study of the nucleon spin structure with high intensity polarized light nuclear beams. The design of the collider allow proton (deuteron) energy up to $\sqrt{s} = 26$ (12) with the average luminosity up to 10^{30} $\text{cm}^{-2}\text{s}^{-1}$.

6 Estimated Cost and Schedule

A serious cost estimate has not been done yet. We expect to use as many of the detector elements and electronics as possible from the FNAL-E906 experiment. The actual cost would depend on how many of the FNAL-E906 equipments could be available. A very rough guess of the cost is on the order of \$3M - \$5M. A cost estimate of the internal target can be given as the cost of the PANDA pellet target which are \$1.5M for R&D and infrastructure, and \$1.5M for the construction. A cost estimate from requirement for accelerator and experimental area (IP2) is the most uncertain part.

One possible rough schedule is:

- 2010 - 2013: FNAL-E906 beam
- 2011 - 2013: R&D of accelerator, and R&D and construction of the internal target

- 2014: experimental setup and commissioning at RHIC
- 2015-2017: phase-1 parasitic experiment (10 weeks \times 3 years)
- 2018: phase-2 dedicated experiment (8 weeks)

References

- [1] D. W. Sivers, *Phys. Rev. D* **41**, 83 (1990).
- [2] V. Barone, A. Drago and P. G. Ratcliffe, *Phys. Rept.* **359**, 1 (2002).
- [3] A. Airapetian *et al.* [HERMES Collaboration], *Phys. Rev. Lett.* **94**, 012002 (2005) [arXiv:hep-ex/0408013].
- [4] V. Y. Alexakhin *et al.* [COMPASS Collaboration], *Phys. Rev. Lett.* **94** (2005) 202002 [arXiv:hep-ex/0503002].
- [5] R. Seidl *et al.* [Belle Collaboration], *Phys. Rev. Lett.* **96**, 232002 (2006) [arXiv:hep-ex/0507063].
- [6] M. Anselmino, M. Boglione, U. D'Alesio, A. Kotzinian, F. Murgia, A. Prokudin and C. Turk, *Phys. Rev. D* **75**, 054032 (2007) [arXiv:hep-ph/0701006].
- [7] J. P. Ralston and D. E. Soper, *Nucl. Phys. B* **152**, 109 (1979).
- [8] M. Gockeler *et al.* [QCDSF Collaboration and UKQCD Collaboration], *Phys. Lett. B* **627**, 113 (2005) [arXiv:hep-lat/0507001].
- [9] A. Airapetian *et al.* [HERMES Collaboration], *Phys. Rev. Lett.* **103**, 152002 (2009) [arXiv:0906.3918 [hep-ex]].
- [10] A. V. Efremov, K. Goeke and P. Schweitzer, *Eur. Phys. J. ST* **162**, 1 (2008) [arXiv:0801.2238 [hep-ph]].
- [11] M. Anselmino *et al.*, *Eur. Phys. J. A* **39**, 89 (2009) [arXiv:0805.2677 [hep-ph]].
- [12] S. J. Brodsky, D. S. Hwang and I. Schmidt, *Phys. Lett.* **530**, 99 (2002); *Nucl. Phys. B* **642**, 344 (2002); J. C. Collins, *Phys. Lett. B* **536**, 43 (2002); X. Ji and F. Yuan, *Phys. Lett. B* **543**, 66 (2002); A. V. Belitsky, X. Ji and F. Yuan, *Nucl. Phys. B* **656**, 165 (2003); D. Boer, P. J. Mulders and F. Pijlman, *Nucl. Phys. B* **667**, 201 (2003).
- [13] A. N. Sissakian, O. Y. Shevchenko, A. P. Nagaytsev and O. N. Ivanov, *Phys. Rev. D* **72**, 054027 (2005) [arXiv:hep-ph/0505214].
- [14] S. Arnold, A. Metz and M. Schlegel, *Phys. Rev. D* **79** (2009) 034005 [arXiv:0809.2262 [hep-ph]].
- [15] A. Bressan [COMPASS Collaboration], arXiv:0907.5508 [hep-ex].
- [16] A. Martin [COMPASS Collaboration], talk presented at DIS2010.
- [17] H. Yokoya, private communications.
- [18] L.Y. Zhu *et al.*, *Phys. Rev. Lett.* **99**, 082301 (2007); **102**, 182001 (2009).
- [19] Z. Lu and I. Schmidt, arXiv:0912.2031 [hep-ph].
- [20] <http://www-panda.gsi.de/>

- [21] M. Anselmino, M. Boglione, U. D'Alesio, S. Melis, F. Murgia and A. Prokudin, Phys. Rev. D **79**, 054010 (2009) [arXiv:0901.3078 [hep-ph]].
- [22] U. D'Alesio and S. Melis, private communications.
- [23] Y. Goto, AIP Conf. Proc. **1149**, 923 (2009).